BIOCHEMISTRY
including biophysical chemistry & molecular biology
Article

Biochemistry **2010,** *49,* 3393–3402 3393
DOI: 10.1021/bi901791x

Insight into the Cellular Uptake Mechanism of a Secondary Amphipathic Cell-Penetrating Peptide for siRNA Delivery[†]

Karidia Konate,[‡] Laurence Crombez,[‡] Sébastien Deshayes,[‡] Marc Decaffmeyer,[§] Annick Thomas,[§] Robert Brasseur,[§] Gudrun Aldrian,[‡] Frederic Heitz,[‡] and Gilles Divita*,[‡]

[‡]*Centre de Recherches de Biochimie Macromoléculaire, CRBM-CNRS, UMR-5237, UM1-UM2, Department of Molecular Biophysics and Therapeutics, University of Montpellier, 1919 Route de Mende, 34293 Montpellier, France, and* [§]*Centre de Biophysique Moléculaire Numérique, Faculté Universitaire des Sciences Agronomiques de Gembloux, Gembloux, Belgium*

Received October 18, 2009; Revised Manuscript Received March 18, 2010

ABSTRACT: Delivery of siRNA remains a major limitation to their clinical application, and several technologies have been proposed to improve their cellular uptake. We recently described a peptide-based nanoparticle system for efficient delivery of siRNA into primary cell lines: CADY. CADY is a secondary amphipathic peptide that forms stable complexes with siRNA and improves their cellular uptake independently of the endosomal pathway. In the present work, we have combined molecular modeling, spectroscopy, and membrane interaction approaches in order to gain further insight into CADY/siRNA particle mechanism of interaction with biological membrane. We demonstrate that CADY forms stable complexes with siRNA and binds phospholipids tightly, mainly through electrostatic interactions. Binding to siRNA or phospholipids triggers a conformational transition of CADY from an unfolded state to an α-helical structure, thereby stabilizing CADY/siRNA complexes and improving their interactions with cell membranes. Therefore, we propose that CADY cellular membrane interaction is driven by its structural polymorphism which enables stabilization of both electrostatic and hydrophobic contacts with surface membrane proteoglycan and phospholipids.

Nowadays, delivery has become a key stone in therapy, since transport across cell membranes remains a serious obstacle in the development of peptide, protein, and nucleic acid based drug therapeutics. Several nonviral technologies have been designed to improve cellular uptake of therapeutic molecules, including electroporation (*1*), liposomes (*2*), polycationic polymers (*3*), nanoparticles (*4*), and peptides (*5*). Among these, cell-penetrating peptides (CPPs)[1] constitute promising alternatives for drug delivery (*6*, *7*) and have been successfully applied to cultured cells and at the preclinical or clinical level (*5*−*14*).

Two main classes of CPPs have been described, the first requiring chemical linkage with the cargo (*6*−*9*) and the second involving the formation of stable, noncovalent complexes (*9*−*12*). Although there is a consensus, as for many carriers, the first contacts between CPPs and the cell surface occur through electrostatic interactions with components of the extracellular matrix, the glucosaminoglycan (GAG) (*15*−*17*). The mechanism through which CPPs promote translocation of active cargoes across plasma membranes is still a matter of debate. For most CPPs, evidence for several routes of cell entry has been reported, and various parameters can drive their cellular uptake pathway, including their structural features and ability to interact with cell membrane components, the nature of the cargo, and the cell membrane composition which is unique to each cell type (*18*−*21*). It is clearly established that the cellular uptake mechanism of CPP-cargo conjugates at low concentration is essentially associated with an energy-dependent endosomal pathway: clathrin- or caveolin-mediated endocytosis or macropinocytosis depending on the cargo (*18*, *19*, *22*, *23*). Systematic comparison of CPPs covalently linked to either fluorophore (*24*) or to splice-correcting peptide−nucleic acid (*23*), a more biologically relevant cargo, has revealed major differences in the efficiency and nature of endosomal pathways. In contrast, at high concentration, uptake of CPP-cargo covalent strategy is partially associated to a nonendosomal process (*25*, *26*). Secondary structure as well as structural polymorphism and dynamics of CPPs plays a major role in cellular uptake of CPP-cargo complexes and in the balance between efficiency and toxicity (*8*), as also mentioned for antimicrobial peptides (*27*). A noncovalent strategy for the delivery of different types of cargo has been proposed based on two families of primary amphipathic peptides, MPG (*28*, *29*) and PEP (*30*, *31*), which form nanoparticles when complexed with cargoes (*10*, *31*−*33*). Both peptides favor cellular uptake through a mechanism that is controlled by the size of the nanoparticles and the ability of the peptide to interact directly with the lipid moiety of the cell membrane (*34*−*37*). The recent discovery that CPPs can trigger membrane repair processes has revealed that the membrane response due to binding or damage associated with CPP interaction can have a major impact on the cellular uptake and efficiency (*38*). Therefore, investigating the impact of CPP folds on cellular uptake mechanisms constitutes an essential piece of the puzzle for their therapeutic development.

We recently described a new peptide-based delivery system for siRNA using the secondary amphipathic peptide CADY (*39*). CADY is a 20-residue peptide, "Ac-GLWRALWRLLRSLWRLLWRA-cya", derived from the chimerical peptide PPTG1 (*40*), a variant of the fusion peptide JTS1 (*41*). In the present work, we

[†]This work was supported in part by the Centre National de la Recherche Scientifique (CNRS) and by grants from the ANR (Agence Nationale de la Recherche, ANR-06-BLAN-0071) and Panomics Inc.

*To whom correspondence should be addressed: tel, +33 (0)4 67 61 33 92; fax, +33 (0)4 67 52 15 59; e-mail, gilles.divita@crbm.cnrs.fr.

[1]Abbreviations: CPP, cell-penetrating peptide; DOPG, dioleylphosphatidylglycerol; DOPC, dioleylphosphatidylcholine; DPPC, dipalmitoylphosphatidylcholine; DPPG, dipalmitoylphosphatidylglycerol; CMC, critical micellar concentration; CD, circular dichroism; GAG, glucosaminoglycan.

Published on Web 03/19/2010

have combined several physicochemical technologies with molecular modeling, circular dichroism, and fluorescence spectroscopy in order to address whether different conformational states of CADY influence association with siRNA-cargo or phospholipids and therefore control cellular uptake. We demonstrate that CADY interacts with both lipids and siRNA tightly, involving both electrostatic and hydrophobic interactions which trigger a conformational transition of CADY to a helical form. Taken together, these results enable us to propose a structure-mediated mechanism of CADY and to identify specific criteria for further design and optimization of CADY peptides.

EXPERIMENTAL PROCEDURES

Materials. Dioleylphosphatidylglycerol (DOPG) and dioleylphosphatidylcholine (DOPC) phospholipids were purchased from Sigma-Aldrich (France), and dipalmitoylphosphatidylcholine (DPPC) and dipalmitoylphosphatidylglycerol (DPPG) were from Avanti Polar Lipids (Alabaster, AL). Heparan sulfate sodium salt extracted from bovine kidney was from Sigma-Aldrich (France).

Peptides. CADY peptide (Ac-GLWRALWRLLRSLWRL-LWRA-cya) was synthesized by solid-phase peptide synthesis using AEDI-expensin resin with (fluorenylmethoxy)carbonyl (Fmoc) continuous (Pionner; Applied Biosystems, Foster city, CA) as described previously (*33*, *42*). CADY was purified by semipreparative reverse-phase high-performance liquid chromatography (RP-HPLC; C18 column Interchrom UP5 WOD/25M Uptisphere 300 5 ODB, 250 mm × 21.2 mm) and identified by electrospray mass spectrometry and amino acid analysis (*28*).

Oligonucleotides. The siRNA and fluorescently labeled siRNA (5′ FAM) were obtained from Eurogentec (Belgium). The different sequences are for anticyclin B1: 5′-CAUCAUCC-CUGCCUCUACUTT-3′ (sense strand). The stock solution of siRNA was prepared in RNase-free water.

Peptide and Phospholipid Liposome Preparations. (*A*) *CADY/siRNA Complex Formation*. Stock solutions of peptide were prepared at 1 mg/mL in distilled water and sonicated for 10 min. CADY/siRNA complexes were formed by incubating CADY peptide (373 μM stock solution) with siRNA (100 μM stock solution) for 30 min at 37 °C.

(*B*) *Preparation of Phospholipid Liposomes*. A mixture of phospholipids in chloroform/methanol solution (3/1) was placed in a rotovapor system to eliminate all of the solvent; then the film of phospholipids was hydrated with distilled water at the required concentration, mixed, and sonicated for 20 min using a Brasson sonicator equipped with a 2×10^{-3} probe (*35*).

Circular Dichroism Measurements. CD spectra were recorded on a JASCO 810 (Tokyo, Japan) dichrograph (*34*, *35*) in a quartz cell with an optical path of 1 mm for peptide in aqueous solutions. Spectra were obtained from three acquisitions between 190 and 260 nm with a data pitch of 0.5 nm, a bandwidth of 1 nm, and a standard sensitivity.

Fluorescence Titrations. Fluorescence experiments were performed on a PTI spectrofluorometer (*39*) at 25 °C in a 154 mM NaCl buffer. Intrinsic Trp fluorescence of CADY was excited at 290 nm, and the emission spectrum was recorded between 310 and 400 nm, with a spectral band-pass of 2 and 8 nm for excitation and emission, respectively. FITC fluorescence of labeled siRNA was excited at 492 nm, and emission was recorded between 500 and 580 nm. For peptide/phospholipid interactions 10 μM peptide or the peptide/siRNA complex was titrated by increasing concentrations of phospholipid vesicles, and fluorescence changes in either Trp or FITC fluorescence were recorded. For the CADY/siRNA interaction 0.5 μM FITC-labeled siRNA was titrated by increasing concentrations of peptide. All measurements were corrected for the dilution, and curve fitting was performed by using Grafit software (Erithacus), as already described (*34*, *43*).

Adsorption and Penetration at the Air−Water Interface. "Monolayer techniques" are potent tools for studying the interfacial properties of membrane-active peptides (*44*, *45*). These methods allow measurements of adsorption and penetration of a peptide. Adsorption consists in the peptide-induced surface pressure ($\Delta\Pi$) at the air−water interface as a function of peptide concentration in the subphase and is therefore indicative of the air−water interface affinity and amphipathic features of peptides (*45*). The maximal concentration for which no further variation of surface pressure is detected corresponds to the critical micellar concentration (CMC) (*45*). Any peptide that can insert into a phospholipid monolayer induces a variation in surface pressure that is indicative of the affinity of the peptide for the monolayer at its insertion into the monolayer. Thus the variation of surface pressure ($\Delta\Pi$) as a function of different initial lipid surface pressures (Πi) allows the extrapolation of the critical pressure of insertion (cpi) which is indicative of the insertion of peptides into phospholipid monolayers (*46*). Adsorption and penetration at the air−water interface were carried out using simultaneously microtrough S with the Film Ware 2.41 from Kibron (Helsinki, Finland) as the analyzer program and an homemade setup in which surface tension was measured with a Prolabo (France) tensiometer using the platinum plate of the Wilhelmy method (*45*). Adsorption test measurements were made at equilibrium after injection of aliquots of an aqueous solution of peptide into the aqueous subphase (0.154 M NaCl solution), gently stirred with a magnetic stirrer. To determine the critical micellar concentration (CMC), this procedure was repeated until no further increase in surface pressure could be detected. For penetration measurements of the peptide into phospholipid monolayers, lipids dissolved in chloroform/methanol solution (3/1 v/v) were spread at room temperature onto the air/phosphate buffer (0.154 M NaCl) solution interface in order to obtain a definite surface pressure. The solvent was allowed to evaporate for at least 15 min, and when a constant surface pressure was reached, a small volume of the aqueous peptide solution was injected into the subphase beneath the lipid monolayer. Increases in surface pressure ($\Delta\Pi$) were recorded for different initial lipid surface pressures (Πi) in order to determine the critical pressure of insertion (cpi) of the peptide into the lipid monolayer (*46*).

Molecular Modeling. Three-dimensional models of CADY were calculated using PepLook software (Biosiris_RA, France). A set of 999 3-D models were sorted as conformations of lower energy among the $(1-2) \times 10^6$ models calculated by the PepLook iterative Boltzman-stochastic procedure using CADY sequence, the CBMN semiempirical force field, and a set of backbone angles calibrated for optimal structure prediction (*47*, *48*). PepLook enables calculation of peptide structural models of structure in several conditions: water, apolar solvent, membrane, and hydrophobicity interface. The interface protocol was used here. Three types of interfaces were used: plain hydrophobicity interface (no charge) and DOPC and DOPG interfaces. In the simulation of interfaces, all energy terms are multiplied by a function $C(z)$ variable along the z axis perpendicular to the

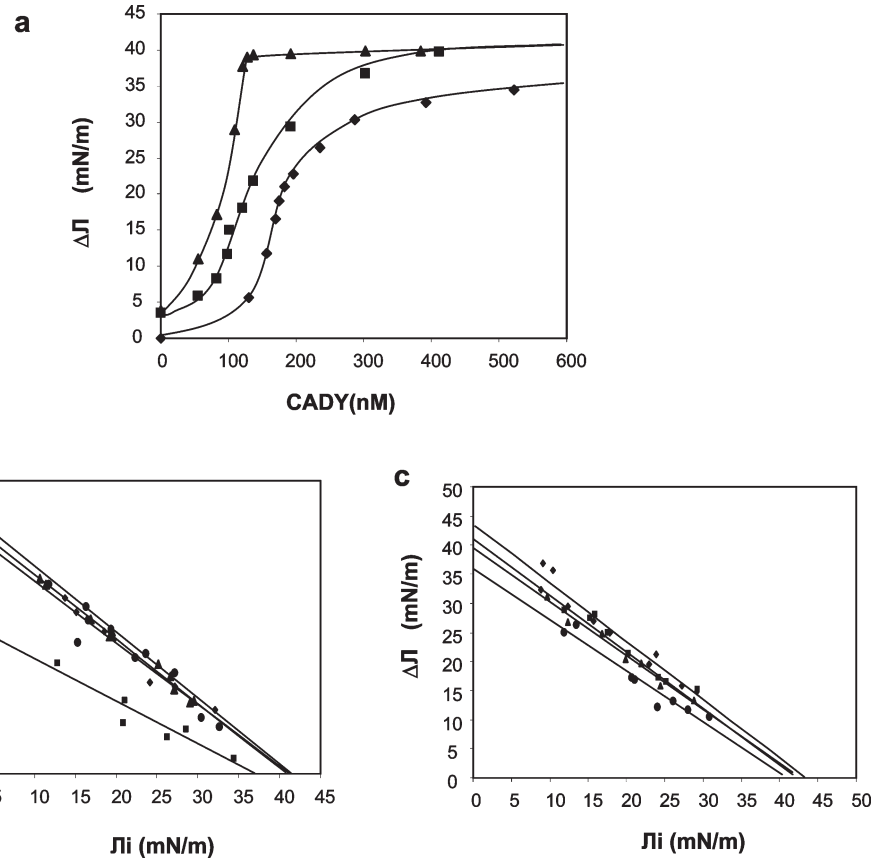

FIGURE 1: Adsorption and penetration of CADY at the air−water interface. (a) Variation of the peptide-induced surface pressure (ΔΠ) as a function of the CADY concentration into the aqueous subphase in the absence (◆) or in the presence of DOPC (■) or DOPG (▲). (b) CADY penetration was monitored by following variation of the surface pressure (ΔΠ) as a function of initial surface pressure (Πi) of the DPPG (◆), DPPC (■), DOPG (▲), or DOPC (●) phospholipid monolayer. (c) Effect of cholesterol on CADY penetration. Penetration was performed by following variation of the surface pressure (ΔΠ) as a function of initial surface pressure (Πi) of the (70/30) DOPC/DOPG phospholipid monolayer containing 0% (●), 10% (◆), 20% (■), and 30% (▲) of DOPC substituted by cholesterol.

interface. $C(z)$ simulates water concentration: its value is 1.0 in water and 0 in apolar media and varies steadily through the interface (*49*). Energy terms used are the hydrophobicity constraint (*49*), the lipid constraint, and, for the DOPC and DOPG interfaces, the electrostatic constraint. This latter constraint is the product of the peptide atom charge by the charge density of lipids divided by the dielectric constant of the medium (80 in water, 3 in a completely apolar medium). The density of charges is calculated across the interface as the sum of all lipid charges, taking into account their relative percentages and their Gaussian distribution of position at all levels of the interface. The compositions of lipids were those used experimentally. The PepLook-selected models are those of minimal intramolecular plus minimal interfacial energies.

Agarose Gel Shift Assay. CADY/siRNA complexes were formed in water; a fixed amount of siRNA (1.7 nmol) was incubated for 30 min at 37 °C with concentrations of CADY corresponding to a peptide/siRNA ratio of 20/1, 40/1, 60/1, and 80/1; then concentrations of HSPG from 0.1 to 10 μg were added to the complex solution. Thirty microliters of each sample, corresponding to 100 pmol of siRNA, was analyzed by electrophoresis on agarose gel (1% w/v) stained with GelRed provided by Biotium Inc. (Canada) and revealed by UV illumination.

RESULTS

Adsorption and Penetration at the Air−Water Interface. We first investigated the potency of CADY to interact with and to penetrate into phospholipid monolayers. As expected from its pronounced amphipathic character; CADY shows a strong affinity for a lipid-free air−water interface (Figure 1a) (*45*). Adsorption of CADY is characterized by a very low critical micellar concentration (CMC) of 230 nM and a high saturating surface pressure of 30 mN/m, values which are extremely high compared to those of other previously described CPPs (<20 mN/m) (*35*, *36*). The presence of phospholipids in the liquid-expanded states (DOPC and DOPG) at low initial pressure significantly decreases the CMC of CADY to 180 nM for DOPC and 100 nM for DOPG, highlighting strong interactions between CADY and phospholipids. To investigate if CADY/phospholipid interactions trigger the insertion of CADY into the phospholipid monolayer, penetration experiments were performed using phospholipids in the liquid-expanded (DOPC and DOPG) and liquid-condensed (DPPG and DPPC) states. CADY concentrations close to the CMC were injected into the subphase, and variations in surface pressure (ΔΠ) were measured from initial pressure values (Πi) which differed slightly between each monolayer spreading. Critical pressure of insertion values (cpi) were estimated by extrapolation of the variation of surface pressure from an initial value of zero (Πi = cpi for ΔΠ = 0) (*46*). As reported in Figure 1b, a similar cpi value of 40−42 mN/m was obtained for DOPC, DOPG, and DPPG, revealing spontaneous insertion of CADY peptide into phospholipid monolayers irrespective of the nature of headgroups (*45*, *46*, *50*). Moreover, the extrapolated variation of surface pressure for an initial pressure of

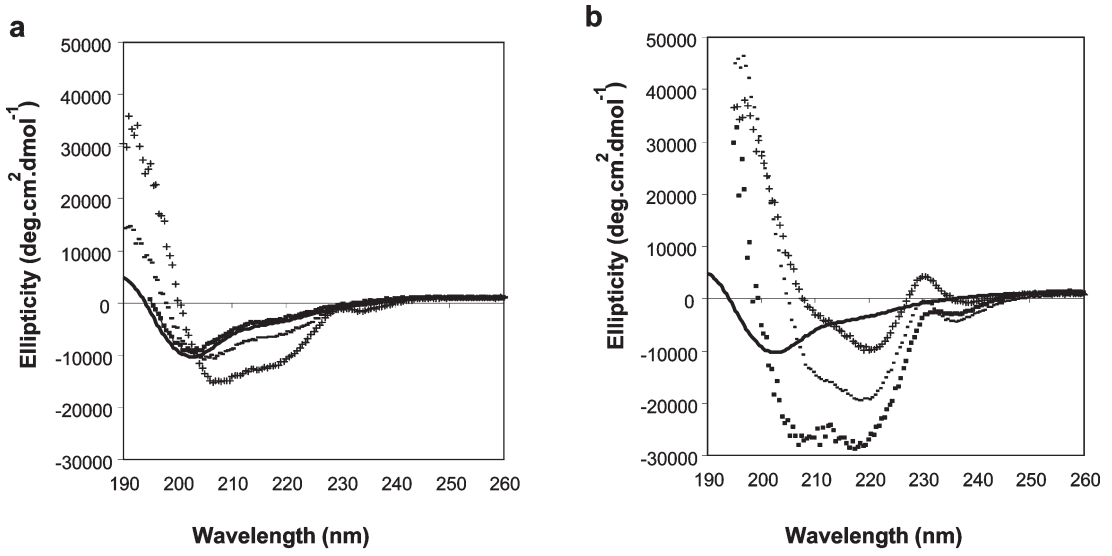

FIGURE 2: Structural analysis of CADY in the presence of phospholipid by circular dichroïsm. Far-UV CD spectra of CADY (50 μM) were measured in the absence (—) or the presence of increasing concentration of DOPC (a) or DOPC (b) phospholipid vesicles. Lipid/CADY ratios of 1/1 (■), 10/1 (- -), and 20/1 (+) were used.

zero ($\Delta\Pi$ for $\Pi i = 0$) (40 mN/m) was higher than that observed for the free peptide at saturation (30 mN/m) (Figure 1b,c), indicative of tight interactions between CADY and the different phospholipids (*45*). In the case of the liquid-condensed DPPC, CADY is able to insert with a high cpi value (~36 mN/m) but the value of surface pressure at low initial pressure (24 mN/m) indicates a limited interaction of CADY with DPPC. These results demonstrate that strong CADY/lipid interactions take place within membrane monolayers, as also reported for the primary amphipathic peptide Pep-1 (*35*). Moreover, cholesterol plays a major role in the control of integrity and fluidity of plasma membranes and has been involved in the cellular uptake mechanism of numerous CPPs (*42*). We investigated the impact of cholesterol on CADY/monolayer interactions. Penetration experiments were performed using mixed monolayers containing DOPC/DOPG (70/30) where DOPC was substituted by different concentrations of cholesterol (10%, 20%, 30%). As shown in Figure 1c, cholesterol does not affect CADY penetration; cpi values are similar in monolayers with and without cholesterol, suggesting no direct interaction of CADY with cholesterol molecules.

Structural Analysis of CADY in its Free and Phospholipid-Associated Forms. The secondary structure of CADY in water was analyzed by circular dichroïsm. For peptide concentrations ranging from 37 to 260 μM, CADY CD spectra exhibit a single minimum centered at 203 nm, characteristic of mainly random coil conformations. To evaluate whether the interaction of CADY with a cell membrane-mimicking environment had any effect on its conformation, the CD spectra of CADY were characterized in the presence of increasing concentrations of phospholipid vesicles. As reported in Figure 2, CADY/phospholipid mixtures show CD spectra typical of helical conformations with two minima at 207 and 222 nm and one maximum around 190 nm, indicating that the presence of either DOPG or DOPC vesicles induces a structural transition of CADY, from random coil to a helical conformation. However, we observed different structural behaviors of CADY depending on the nature of the phospholipids. In the presence of DOPC, CADY conformational changes of CADY are optimal for a DOPC/peptide ratio of 20/1 (Figure 2a), whereas the transition of CADY conformation from random to α-helix is achieved at a 1/1 CADY/DOPG ratio. Increasing concentrations of DOPG result in a deformation of the CD spectrum characterized by a modification of the 222/207 nm ratio and an increase of the band at 228 nm. The ratio of intensities at 222 and 207 nm can be used to distinguish coiled coils from isolated helices (≥ 1 for coiled coils and < 0.86 for isolated helices (*51*)). Thus the modification of this ratio suggests an increase in helical content and probably helix aggregation. The increase in the band at 228 nm can be associated with the contribution of the 4-Trp of CADY upon insertion into phospholipids or to electrostatic interactions between CADY and phospholipids (Figure 2b).

CADY/Phospholipid Interactions As Monitored by Fluorescence Spectroscopy. Interactions between CADY and phospholipid vesicles were analyzed by intrinsic fluorescence spectroscopy. CADY peptide contains four Trp residues that constitute very sensitive intrinsic probes. As reported in Figure 3, binding of CADY to liposome results in a Trp fluorescence emission blue shift of 17 and 13 nm, associated with a 1.8- and 2-fold increase in fluorescence intensity in the presence of DOPG and DOPC, respectively (data not shown), indicating a change in the environment of Trp residues from polar to apolar. The more pronounced shift observed for DOPG (345−328 nm) in comparison to DOPC (345−332 nm) can be associated with additional electrostatic interactions of CADY with the charged phospholipids, which modify the environment of Trp residues by, for instance, affecting the relative orientation of CADY within lipids. Titration experiments reveal than both DOPC and DOPG induce a fluorescence shift with a similar saturation for a lipid/peptide molar ratio of about 3 (Figure 3b), thereby confirming that the nature of phospholipid headgroups has no influence on the fluorescence changes of Trp.

In Silico Structural Modeling of CADY. We previously proposed using PepLook that CADY adopts a secondary amphipathic helical conformation within membrane-mimicking environments, exposing Trp groups on one side, charged residues on the other, and hydrophobic residues on yet another (*39*). In order to better understand the structural variations triggered by peptide/lipid interactions, the structure of CADY was modeled in three different interfacial conditions: in water, in an uncharged

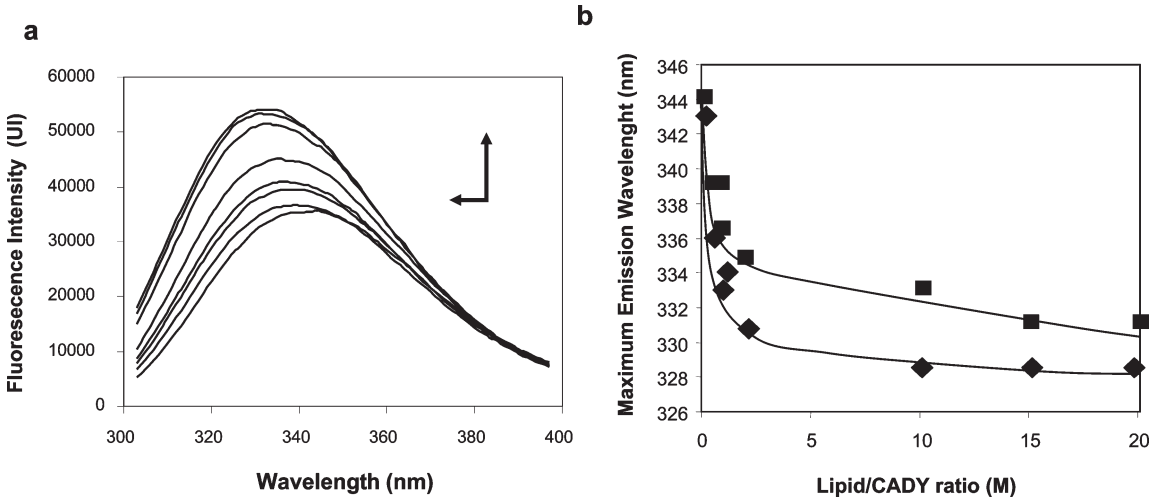

FIGURE 3: Effect of the addition of phospholipid vesicles on the fluorescence on the Trp residues of CADY. (a) CADY (10 μM) was titrated by increasing concentrations of DOPG, Trp fluorescence was excited at 290 nm, and the emission spectrum was recorded between 310 and 400 nm. (b) Variation of the CADY fluorescence emission wavelength as a function of the ratio of DOPC/peptide (■) or of DOPG/peptide (◆).

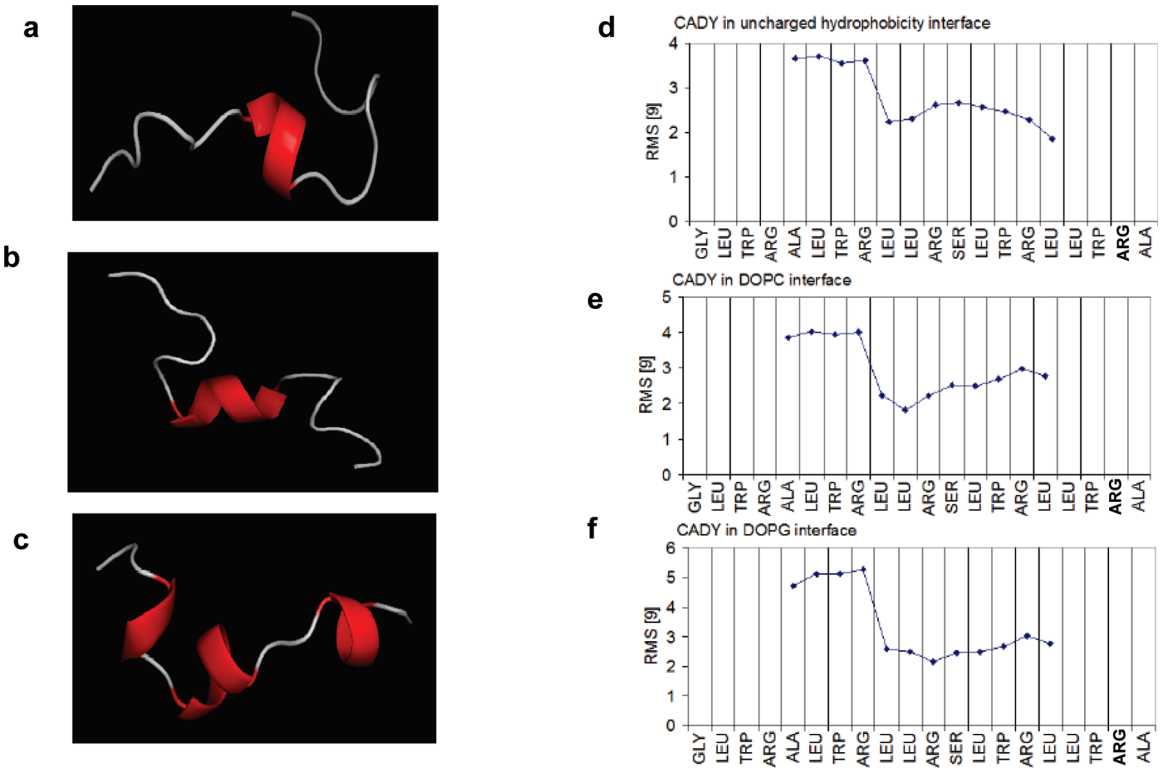

FIGURE 4: CADY structures in different interfacial environments. The structures of CADY were calculated using Peplook software in three types of interfaces: (a) hydrophobicity interface (no charge), (b) DOPC layer interface, and (c) DOPG layer interface. Plots of the averaged RMSD of the 998 low energy models versus the prime (lower energy model) on a window of nine residues along the sequence for mapping the polymorphism variability at (d) hydrophobicity, (e) DOPC layer, and (f) DOPG layer interfaces.

hydrophobic interface, and in a DOPC and a DOPG interface using the same PepLook software (*47*, *48*). In water, CADY does not adopt any specific secondary structure in agreement with the random coil detected in CD experiments. In contrast, at an hydrophobic interface, the lowest energy model of CADY exhibits 20% of helical secondary structure corresponding to the central "RLLR" motif (Figure 4a). In DOPC and DOPG interfaces, the lowest energy model of CADY (the prime) is 30% and 60% helical, respectively (Figure 4b,c). In the presence of DOPC the helical motif involves mainly the central "RLLRSL" motif. In DOPG, in addition to the "RLLRS" central core, ^{4}RAL^{7} and ^{16}RLLW^{19} residues also fold into a helical conformation, suggesting that negatively charged lipids stabilize the helical fold of CADY, in perfect agreement with CD and penetration measurements. The structural polymorphism of CADY in the different environments was evaluated by analyzing the averaged root mean square deviation (RMSD) on a window of nine amino acids of the 998 additional low-energy structural models versus the "prime". As reported in Figure 4d−f, irrespective of the environment, CADY major structural variations take place at its N-terminus, with a transition at the central "RLLR" motif which always adopts a helical structure (Figure 4c), while the rest of the

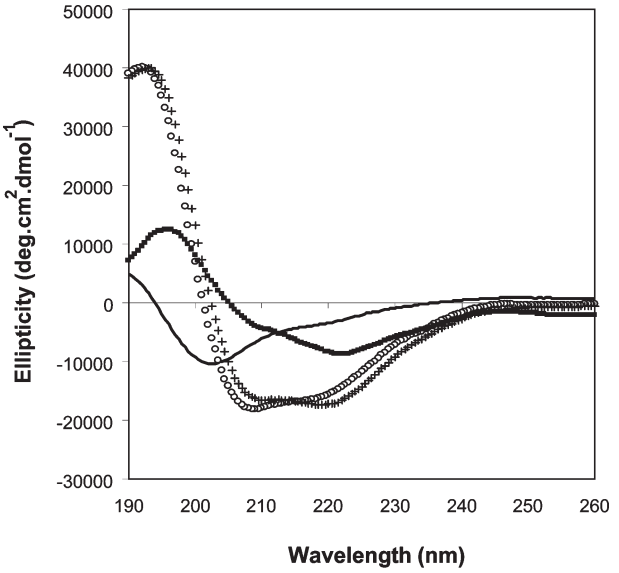

FIGURE 5: Influence of the interaction with siRNA on the structure of CADY. Far-UV CD spectra of CADY (50 μM) were measured in the absence (—) and in the presence of siRNA peptide/oligonucleotide ratios of 40/1 (○), 20/1 (+), and 10/1 (■).

peptide is less polymorphic. These results infer that CADY has a marked structural polymorphism and can therefore adopt different conformational states.

SiRNA-Mediated Conformational Changes of CADY. We previously demonstrated that CADY forms stable complexes with siRNA and improves their delivery into several challenging cell lines (*39*). We therefore evaluated the impact of a small interfering RNA (21/21 mer) on the secondary structure of CADY by CD. As reported in Figure 5, upon binding to siRNA, CADY exhibits a CD spectrum typical of helical conformation with two minima at 207 and 222 nm and one maximum around 190 nm. We found that the helical fold of CADY is dependent on the concentration of siRNA with a maximum for a peptide/siRNA molar ratio of 40/1. At a lower molar ratio (10/1), the presence of a large ratio of oligonucleotide versus CADY leads to a deformation of the CD spectra with a decrease in the ellipticity at 207 nm and an increase at 222 nm, which might be related to the spectral contribution of the double-stranded siRNA and/or to electrostatic interactions and helix aggregation as observed in the presence of DOPG. It should be noted here that the spectrum of free siRNA in solution does not undergo any change in the presence of vesicles (data not shown).

Interactions of CADY/siRNA with Phospholipids As Monitored by Fluorescence Spectroscopy. Binding and insertion of CADY into phospholipids are associated with a blue shift of the maximum wavelength of Trp fluorescence. As reported in Figure 6a, similar experiments performed with the CADY/siRNA complex at 20/1 molar ratio also pointed to a lipid concentration-dependent fluorescence emission with a blue shift from 340 to 329 nm and to 331 nm for DOPG and DOPC, respectively. In both DOPC and DOPG, CADY/siRNA complex binding saturation is achieved at a lipid/peptide ratio of about 3/1 (Figure 3b), These results demonstrate direct interactions between the CADY/siRNA complex and phospholipids, which are similar to those of free CADY.

The interaction of CADY/siRNA was investigated using fluorescently labeled siRNA (FITC-siRNA). CADY binding to FITC-labeled siRNA induces 70−90% quenching of FITC fluorescence depending on CADY concentration. Titration curves reported in Figure 6a (insert) show that saturation was achieved at a CADY/siRNA ratio of 12 ± 2, with an estimated dissociation constant of 47 ± 10 nM, values which are in perfect agreement with the fact that one siRNA molecule interacts with more than one molecule of CADY, as previously described (*39*). As reported in Figure 6b, interaction of the CADY/FITC-siRNA complex with phospholipid vesicles induces changes in FITC fluorescence. Upon binding to DOPG, siRNA fluorescence is increased by approximately 120%, 80%, and 70% for peptide/siRNA molar ratios of 80, 40, and 20, respectively. In all cases, saturation is achieved at a lipid/CADY molar ratio of 3/1, as already observed for intrinsic Trp fluorescence, indicating that similar interaction and/or insertion mechanisms are monitored by the two fluorescence approaches and that the CADY/siRNA complex remains stable upon interaction with phospholipids. The increase in FITC fluorescence can be associated either to partial uncoating of the siRNA due to peptide/lipid interactions or to changes in the siRNA environment.

Binding of CADY to siRNA Alters Its Adsorption Property at the Air−Water Interface. As CADY delivery is based on the formation of stable complexes with cargoes, the impact of the peptide/siRNA complex on the air−water interface adsorption curves was investigated. CADY/siRNA complexes were prepared by incubating peptide/siRNA ratios of 20/1, 40/1, and 80/1 using a fixed siRNA concentration (3 μM) and varying CADY concentrations, in water for 30 min at 37 °C, and then injected into a saline solution as subphase. As reported in Figure 7, the surface pressure increased only for the 80/1 peptide/siRNA ratio, not for the lower ratios (20/1 and 40/1). As for free CADY, the adsorption of the 80/1 ratio sample was characterized by a low CMC of 400 nM (CMC = 230 nM for free CADY) and a high saturating surface pressure of 30 mN/m. These results demonstrate the presence of highly stable complexes in solution, mainly due to electrostatic interactions between cationic residues of CADY and anionic charges of the phosphate backbone of siRNA, which at low peptide/siRNA ratios trap most of the peptide. In contrast, at the higher ratio of 80/1 siRNA negative charges are overcompensated by peptide positive charges, and the excess of CADY can be involved in peptide/peptide interactions that confer to the complex the ability to adsorb at the interface.

Formation of CADY/siRNA Complexes Involves Mainly Electrostatic Interactions. In order to better understand the behavior of the CADY/siRNA complexes within the cell membrane environment, we evaluated the impact of charged proteoglycan on complex stability. The stability of CADY/siRNA complexes at different molar ratios (20/1−80/1) in the presence of HSPG was analyzed by electrophoresis on agarose gel. As reported in Figure 8, in all cases, CADY/siRNA complexes are extremely stable in the absence of HSPG, and the siRNA remains associated to the peptide at low concentrations of HSPG (0.1 μg). Incubation with higher concentrations of HSPG dissociates the CADY/siRNA complexes and restores incorporation of siRNA in the gel. Complex dissociation is dependent on both the CADY/siRNA ratio and the concentration of HSPG (Figure 8). For peptide/siRNA molar ratios ranging from 20/1 to 60/1, complex destabilization by HSPG is concentration-dependent and optimal for 10 μg of HSPG. In contrast, peptide/siRNA complexes at a molar ratio of 80/1 are highly stable, and even high concentrations of HSPG (10 μg) barely dissociate the complex.

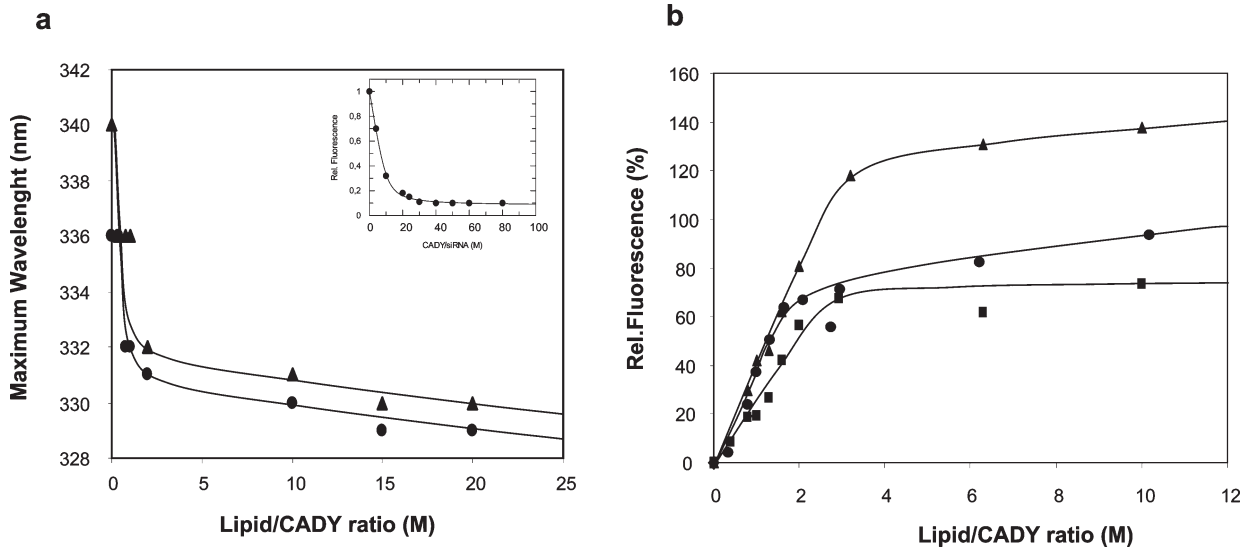

FIGURE 6: Impact of phospholipid vesicles on CADY/siRNA complexes. CADY/siRNA complexes were formed at a molar ratio of 20/1. (a) Effect of phospholipid vesicles on the fluorescence on the Trp residues of CADY in complex with siRNA. CADY/siRNA complexes were titrated by increasing concentrations of DOPG (▲) and DOPC (●), Trp fluorescence was excited at 290 nm, and the emission spectrum was recorded between 310 and 400 nm. The variation of the CADY fluorescence emission wavelength is plotted as a function of the ratio of DOPC/peptide or of DOPG/peptide. (Insert) Formation of the CADY/siRNA complex monitored by FITC-siRNA extrinsic fluorescence. FITC-labeled siRNA was titrated by increasing concentrations of CADY, and the change in FITC fluorescence emission was measured at 512 nm. (b) Binding of CADY/siRNA complexes to phospholipid vesicles measured by extrinsic fluorescence. FITC fluorescence was excited at 492 nm, and emission was measured at 512 nm. CADY/siRNA complexes obtained at ratios of 80/1 (◆), 40/1 (■), and 20/1 (▲) were titrated by increasing concentrations of DOPG.

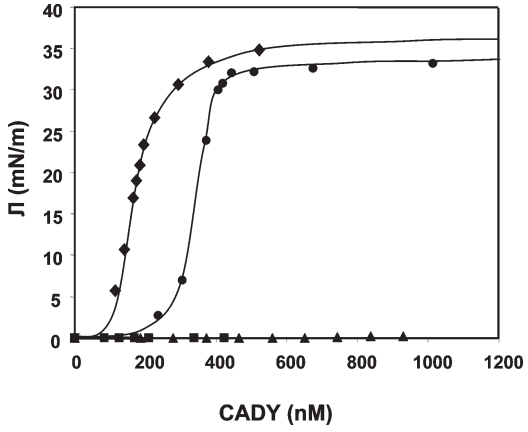

FIGURE 7: Adsorption experiments of the CADY/siRNA complex at the air−water interface. Variation of the peptide-induced surface pressure as a function of the CADY concentration into the aqueous subphase in the absence of siRNA (◆) or at different peptide/oligonucleotide ratios: 80/1 (●), 40/1 (▲), and 20/1 (■).

DISCUSSION

Amphipathic peptide-based noncovalent strategy has been reported as an interesting alternative to chemical coupling for the delivery of different types of cargoes *ex vivo* and *in vivo* (*7*, *10*, *12*), and it appears to be more appropriate for siRNA delivery, yielding significant associated biological response (*5*, *12*, *33*, *52*). We recently proposed a new secondary amphipathic peptide, "CADY", that forms stable complexes with siRNA through electrostatic contacts and improves cellular uptake of biologically active siRNA in a large variety of challenging cell lines via a mechanism independent of the endosomal pathway (*39*). In the present study, we demonstrate that CADY interactions with lipids and siRNA trigger a conformational transition of CADY to a helical form and that this structural polymorphism plays a critical role in its mechanism of interaction with the biological membrane.

Structural Polymorphism of CADY Plays a Major Role in Membrane Insertion. Surface pressure and fluorescence measurements indicate that CADY can spontaneously insert into lipid monolayers and bilayers used as membrane models, irrespective of the nature of phospholipids, of their net charge (neutral PC vs anionic PG), and of their physical state (unsaturated DO vs saturated DP). Both approaches show that CADY exhibits a high affinity for DPPG, DOPC, and DOPG with a similar cpi of 42 mN/m and a binding saturation at a lipid/peptide molar ratio of 3/1. CADY insertion into membranes involves hydrophobic and electrostatic contacts. Interactions are predominantly initiated by the hydrophobicity of CADY, followed by interactions between the cationic charges of the four Arg and the Lys residues of CADY, and the polar head groups of anionic lipids, which stabilize its conformation within the membrane. The secondary structure of amphipathic peptides and their structural versatility play major roles in the mechanism of cellular uptake (*26*, *34*, *35*, *39*). Therefore, characterization of the conformational changes CADY undergoes upon binding to cargo or to membrane components is essential to understand the mechanism underlying cellular uptake of CADY/siRNA complexes, as well as to identify parameters to control CADY efficiency. In contrast to PPTG1 (*40*) or Pep-1 (*35*), which adopt a helical structure in water, CADY peptide is poorly structured and has a low tendency to self-associate, at least in the range of concentrations used in this study. Binding to phospholipid vesicles triggers a conformational transition of CADY from random coil to an α-helix, inducing segregation along the helical axis of charged residues, aromatic residues, and hydrophobic residues. Although CADY binds phospholipids with high affinity, irrespective of their nature, its helical fold differs for DOPC and DOPG. PepLook-calculated models of CADY show that the helical content is dependent on the environment and increases from less than 5% in water to 20% at a hydrophobic interface and to 30% and 60% in the presence of DOPC or DOPG, respectively. In all

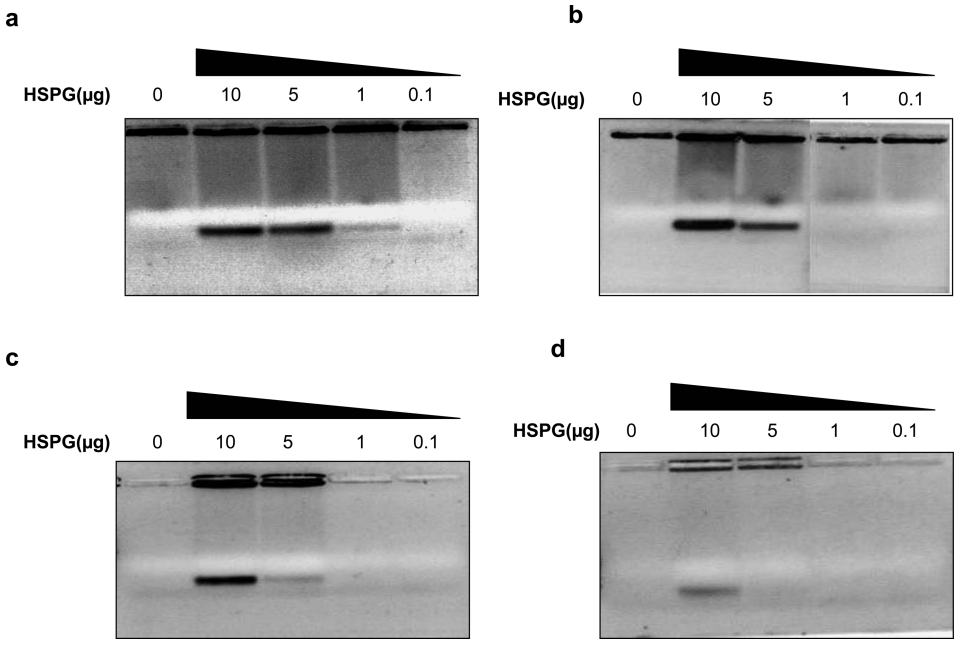

FIGURE 8: CADY interacts with siRNA and heparan sulfate. A fixed siRNA concentration of 0.33 nmol was incubated for 30 min at 37 °C in water with increasing molar ratios of CADY: 20/1 (a), 40/1 (b), 60/1 (c), and 80/1 (d). After complex formation increasing concentrations of heparan sulfate were added to the complexes. Samples were analyzed by electrophoresis on a 1% agarose gel, stained with GelRed, and revealed by UV illumination.

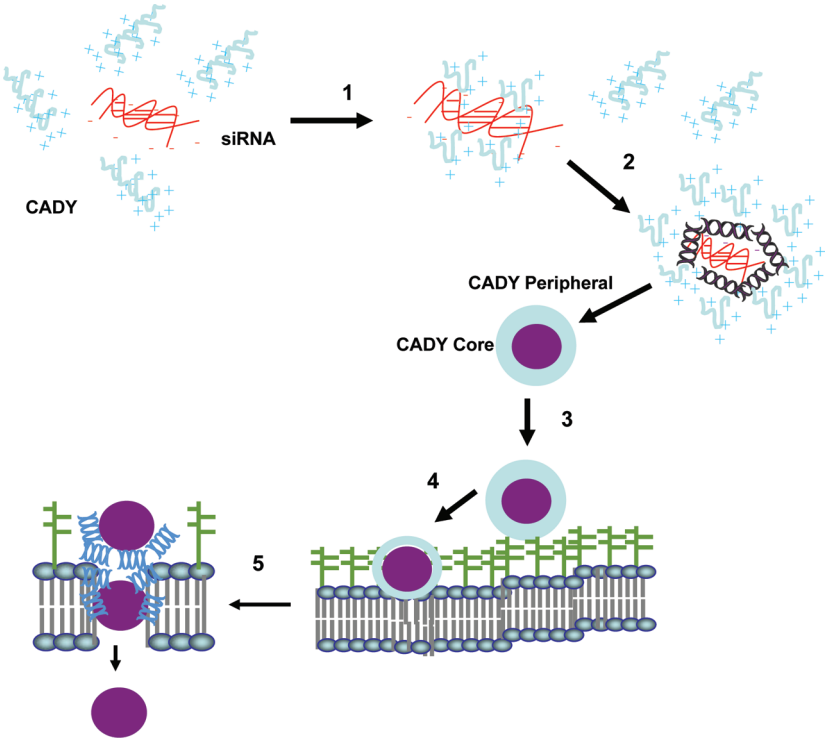

FIGURE 9: Schematic model for the formation and internalization of CADY/siRNA particles. The four steps correspond to (1) electrostatic interactions between siRNA and CADY, which initiated a partial helical folding of CADY to form the core of the complex (purple), (2) stabilization of the CADY/siRNA complex by CADY/CADY interactions, corresponding to CADY peripheral, (3) electrostatic interaction of CADY/siRNA complexes with cell surface proteoglycan, (4) followed by interaction with phospholipids, and (5) then insertion into the cell membrane mediated by the CADY peripheral and release into the cytoplasmic side of the core complex.

hydrophobic media, the central "RLLRSL" motif of CADY initiates the helical structure; then electrostatic interactions increase and stabilize the helical conformation at both the N- and C-terminus by decreasing the repulsion between arginine residues (Figure 4). Interestingly, the helix-inducing effect by DOPG gives rise to a deformation in the CD spectrum with an increase in ellipticity at 207, 222, and 228 nm that can be attributed to helix aggregation, as described by Lau et al. (*51*), or to changes in the orientation of the helix which may be perpendicular to the membrane plane, as already proposed for numerous proteins or peptides containing transmembrane helical domains (*54*).

Stable CADY/siRNA Complexes Penetrate the Phospholipid Membrane. CADY forms stable complexes with siRNA, with high affinity and that first involve electrostatic interactions between Arg/Lys of CADY and phosphate groups of the siRNA, which is followed by an implication of the Trp residues in the stabilization of the CADY/siRNA complex. We previously demonstrated that CADY peptide promotes cellular uptake of small oligonucleotides but not of large plasmid DNA, in contrast to its parental peptide PPTG1 (*40*). Conversely, PPTG1 was reported to deliver large plasmid molecules into cells but not siRNA delivery (*40*). Interestingly, the presence of Trp is the major difference between CADY and PPTG1 sequences, suggesting that Trp residues are essential to stabilize interactions with small siRNA, whereas electrostatic interactions are involved in complexation of large DNA by PPTG1. Also, the fact that PPTG1 presents a major helical fold in solution, but not CADY, emphasizes the importance of the structural versatility of CADY, which provides greater flexibility during interaction with siRNA, which in turn triggers helical folding of CADY.

Model for CADY Cellular Uptake Mechanism. In contrast to numerous CPPs, CADY, like MPG and Pep-1, spontaneously inserts into natural membranes and exhibits a marked structural polymorphism/versatility, both of which are critical parameters for cellular uptake (*34*). Upon interaction with lipids, these peptides adopt a helical (Pep-1, CADY) and a β-structure (MPG), which has been associated with transient membrane destabilization favoring translocation of CPP-cargo complexes. In contrast, commonly used CPPs such as TAT and Arg_9 do not adopt any secondary structure either in solution or in the presence of lipids and therefore enter the cell mainly by endocytosis (*18*, *19*, *23*). Similarly, penetratin does not present any amphipathic properties, and its structural state seems to be highly dependent on the experimental conditions including the nature of the lipids, concentrations, and the cargo (*53*, *55*). Taking into account the different results on CADY (ref *39*, this work), we propose the following working model for the formation and internalization of CADY/siRNA particles (Figure 9). First, formation of CADY/siRNA particles involves mainly electrostatic interactions between siRNA and Arg, which are stabilized by the implication of the Trp residues. Binding of CADY to siRNA initiates the helical folding of CADY or increases the probability of a preexisting helical conformation. Second, stable CADY/siRNA complexes establish electrostatic interactions with proteoglycans at the cell surface and/or phospholipids. This mechanistic step is dependent on the CADY/siRNA molar ratio, suggesting the presence of a core particle containing CADY molecules in direct contact with siRNA, covered by a more dynamic layer of CADY molecules that form peptide/peptide interactions and interact with GAG and phospholipids. At low molar ratios (20/1), CADY peptides are essentially involved in electrostatic interactions with siRNA forming the "core" of the complex. In contrast, at a molar ratio of 80/1, several CADY molecules forming the peripheral layer of the complex are directly accessible to interact with phospholipids. Third, stable CADY/siRNA complexes interact with the phospholipid phase of the membrane and trigger membrane disorganization, which favors cellular uptake of the siRNA independently of the endosomal pathway.

ACKNOWLEDGMENT

We thank May C. Morris (CRBM-UMR5237-CNRS) for critical reading of the manuscript and all members of the laboratory for fruitful discussions.

REFERENCES

1. Cemazar, M., Golzio, M., Sersa, G., Rols, M. P., and Teissié, J. (2006) Electrically-assisted nucleic acids delivery to tissues in vivo: where do we stand? *Curr. Pharm. Des. 12*, 3817–3825.
2. Torchilin, V. P. (2005) Recent advances with liposomes as pharmaceutical carriers. *Nat. Rev. Drug Discovery 4* (2), 145–60.
3. Ogris, M., and Wagner, E. (2002) Targeting tumors with non-viral gene delivery systems. *Drug Discovery Today 7*, 479–485.
4. Whitehead, K. A., Langer, R, and Anderson, D. G. (2009) Knocking down barriers: advances in siRNA delivery. *Nat. Rev. Drug Discovery 8*, 129–138.
5. Heitz, F., Morris, M. C., and Divita, G. (2009) Twenty years of cell-penetrating peptides: from molecular mechanisms to therapeutics. *Br. J. Pharmacol. 157*, 195–206.
6. El-Andaloussi, S., Holm, T., and Langel, U. (2005) Cell-penetrating peptides:mechanism and applications. *Curr. Pharm. Des. 11*, 3597–3611.
7. Morris, M. C., Deshayes, S., Heitz, F., and Divita, G. (2008) Cell-penetrating peptides: from molecular mechanisms to therapeutics. *Biol. Cell 100*, 201–217.
8. Deshayes, S., Morris, M., Heitz, F., and Divita, G. (2008) Delivery of proteins and nucleic acids using a non-covalent peptide-based strategy. *Adv. Drug Delivery Rev. 260*, 537–547.
9. Murriel, C. L., and Dowdy, S. F. (2006) Influence of protein transduction domains on intracellular delivery of macromolecules. *Expert Opin. Drug Delivery 3*, 739–746.
10. Gros, E., Deshayes, S., Morris, M. C., Aldrian-Herrada, G., Depollier, J., Heitz, F., and Divita, G. (2006) A non-covalent peptide-based strategy for protein and peptide nucleic acid delivery. *Biochim. Biophys. Acta 1758*, 384–393.
11. Meade, B. R., and Dowdy, S. F. (2007) Exogenous siRNA delivery using peptide transduction domains/cell penetrating peptides. *Adv. Drug Delivery Rev. 59*, 134–140.
12. Crombez, L., Morris, M. C., Deshayes, S., Heitz, F., and Divita, G. (2008) Peptide-based nanoparticle for ex vivo and in vivo drug delivery. *Curr. Pharm. Des. 14*, 3656–3665.
13. Dietz, G. P., and Bähr, M. (2004) Delivery of bioactive molecules into the cell: the Trojan horse approach. *Mol. Cell. Neurosci. 27*, 85–131.
14. Foerg, C., and Merkle, H. P. (2008) On the biomedical promise of cell penetrating peptides: limits versus prospects. *J. Pharm. Sci. 97*, 144–162.
15. Gerbal-Chaloin, S., Gondeau, C., Aldrian-Herrada, G., Heitz, F., Gauthier-Rouvière, C., and Divita, G. (2007) First step of the cell-penetrating peptide mechanism involves Rac1 GTPase-dependent actin-network remodelling. *Biol. Cell 99*, 223–238.
16. Duchardt, F., Fotin-Mleczek, M., Schwarz, H., Fischer, R., and Brock, R. (2007) A comprehensive model for the cellular uptake of cationic cell-penetrating peptides. *Traffic 8*, 848–66.
17. Ziegler, A. (2008) Thermodynamic studies and binding mechanisms of cell-penetrating peptides with lipids and glycosaminoglycans. *Adv. Drug Delivery Rev. 60*, 580–597.
18. Richard, J. P., Melikov, K., Vives, E., Ramos, C., Verbeure, B., Gait, M. J., Chernomordik, L. V., and Lebleu, B. (2003) Cell-penetrating peptides. A reevaluation of the mechanism of cellular uptake. *J. Biol. Chem. 278*, 585–590.
19. Wadia, J. J., Stan, R. V., and Dowdy, S. (2004) Transducible TAT-HA fusogenic peptide enhances escape of TAT-fusion proteins after lipid raft macropinocytosis. *Nat. Med. 10*, 310–315.
20. Nakase, I.; et al. (2007) Interaction of arginine-rich peptides with membrane-associated proteoglycans is crucial for induction of actin organization and macropinocytosis. *Biochemistry 46*, 492–450.
21. Padari, K., Saalik, P., Hansen, M., Koppel, K., Raid, R., Langel, U., and Pooga, M. (2005) Cell transduction pathways of transportans. *Bioconjugate Chem. 16*, 1399–1410.
22. El Andaloussi, S., Johansson, H. J., Holm, T., and Langel, U. (2007) A novel cell-penetrating peptide, M918, for efficient delivery of proteins and peptide nucleic acids. *Mol. Ther. 15*, 1820–1826.
23. Lundin, P., Johansson, H., Guterstam, P., Holm, T., Hansen, M., Langel, U., and El Andaloussi, S. (2008) Distinct uptake routes of cell-penetrating peptide conjugates. *Bioconjugate Chem. 19*, 2535–2542.
24. Mueller, J., Kretzschmar, I., Volkmer, R., and Boisguerin, P. (2008) Comparison of cellular uptake using 22 CPPs in 4 different cell lines. *Bioconjugate Chem. 19*, 2363–2374.
25. Fretz, M. M., Penning, N. A., Al-Taei, S., Futaki, S., Takeuchi, T., Nakase, I., Storm, G., and Jones, A. T. (2007) Temperature-, concentration- and cholesterol-dependent translocation of L- and D-octa-arginine across the plasma and nuclear membrane of CD34+ leukaemia cells. *Biochem. J. 403*, 335–342.

26. Su, Y., Mani, R., Doherty, T., Waring, A. J., and Hong, M. (2008) Reversible sheet-turn conformational change of a cell-penetrating peptide in lipid bilayers studied by solid-state NMR. *J. Mol. Biol. 381*, 1133–1144.
27. Henriques, S. T., Melo, M. N., and Castanho, M. A. (2006) Cell-penetrating peptides and antimicrobial peptides: how different are they? *Biochem. J. 399*, 1–7.
28. Morris, M. C., Vidal, P., Chaloin, L., Heitz, F., and Divita, G. (1997) A new peptide vector for efficient delivery of oligonucleotides into mammalian cells. *Nucleic Acids Res. 25*, 2730–2736.
29. Simeoni, F., Morris, M. C., Heitz, F., and Divita, G. (2003) Insight into the mechanism of the peptide-based gene delivery system MPG: implications for delivery of siRNA into mammalian cells. *Nucleic Acids Res. 31*, 2717–2724.
30. Morris, M. C., Depollier, J., Mery, J., Heitz, F., and Divita, G. (2001) A peptide carrier for the delivery of biologically active proteins into mammalian cells. *Nat. Biotechnol. 19*, 1173–1176.
31. Morris, M. C., Gros, E., Aldrian-Herrada, G., Choob, M., Archdeacon, J., Heitz, F., and Divita, G. (2007) A non-covalent peptide-based carrier for in vivo delivery of DNA mimics. *Nucleic Acids Res. 35*, e49–e59.
32. Munoz-Morris, M. A., Heitz, F., Divita, G., and Morris, M. C. (2007) The peptide carrier Pep-1 forms biologically efficient nanoparticle complexes. *Biochem. Biophys. Res. Commun. 355*, 877–882.
33. Crombez, L., Morris, M. C., Dufort, S., Aldrian-Herrada, G., Nguyen, Q., Mc Master, G., Coll, J. L., Heitz, F., and Divita, G. (2009) Targeting cyclin B1 through peptide-based delivery of siRNA prevents tumour growth. *Nucleic Acids Res. 37*, 4559–4569.
34. Deshayes, S., Morris, M. C., Divita, G., and Heitz, F. (2005) Cell-penetrating peptides: tools for intracellular delivery of therapeutics. *Cell. Mol. Life Sci. 62*, 1839–1849.
35. Deshayes, S., Heitz, A., Morris, M. C., Charnet, P., Divita, G., and Heitz, F. (2004) Insight into the mechanism of internalization of the cell-penetrating carrier peptide Pep-1 through conformational analysis. *Biochemistry 43*, 1449–1457.
36. Deshayes, S., Gerbal-Chaloin, S., Morris, M. C., Aldrian-Herrada, G., Charnet, P., Divita, G., and Heitz, F. (2004) On the mechanism of non-endosomial peptide-mediated cellular delivery of nucleic acids. *Biochim. Biophys. Acta 1667*, 141–147.
37. Deshayes, S., Plénat, T., Aldrian-Herrada, G., Divita, G., Le Grimellec, C., and Heitz, F. (2004) Primary amphipathic cell-penetrating peptides: structural requirements and interactions with model membranes. *Biochemistry 43*, 7698–7706.
38. Palm-Apergi, C., Lorents, A., Padari, K., Pooga, M., and Hällbrink, M. (2009) The membrane repair response masks membrane disturbances caused by cell-penetrating peptide uptake. *FASEB J. 23*, 214–223.
39. Crombez, L., Aldrian-Herrada, G., Konate, K., Nguyen, Q. N., Mc Master, G. K., Brasseur, R., Heitz, F., and Divita, G. (2009) A new potent secondary amphipathic cell-penetrating peptide for siRNA delivery into mammalian cells. *Mol. Ther. 17*, 95–103.
40. Rittner, K., Benavente, A., Bompard-Sorlet, A., Heitz, F., Divita, G., Brasseur, R., and Jacobs, E. (2002) New basic membrane-destabilizing peptides for plasmid-based gene delivery in vitro and in vivo. *Mol. Ther. 5*, 104–114.
41. Gottschalk, S.; et al. (1996) A novel DNA-peptide complex for efficient gene transfer and expression in mammalian cells. *Gene Ther. 3*, 448–453.
42. Fittipaldi, A., Ferrari, A., Zoppe, M., Arcangeli, C., Pellegrini, V., Beltram, F., and Giacca, M. (2003) Cell membrane lipid rafts mediate caveolar endocytosis of HIV-1 Tat fusion proteins. *J. Biol. Chem. 278*, 34141–34149.
43. Morris, M. C., Chaloin, L., Mery, J., Heitz, F., and Divita, G. (1999) A novel potent strategy for gene delivery using a single peptide vector as a carrier. *Nucleic Acids Res. 27*, 3510–3517.
44. Brockman, H. (1999) Lipid monolayers: why use half a membrane to characterize protein-membrane interactions? *Curr. Opin. Struct. Biol. 9*, 438–443.
45. Maget-Dana, R. (1999) The monolayer technique: a potent tool for studying the interfacial properties of antimicrobial and membrane-lytic peptides and their interactions with lipid membranes. *Biochim. Biophys. Acta 1462*, 109–140.
46. Calvez, P., Bussières, S., Demers, E., and Salesse, C. (2009) Parameters modulating the maximum insertion pressure of proteins and peptides in lipid monolayers. *Biochimie 91*, 718–733.
47. Thomas, A., Deshayes, S., Decaffmeyer, M., Van Eyck, M. H., Charloteaux, B., and Brasseur, R. (2006) Prediction of peptide structure: how far are we? *Proteins 65*, 889–897.
48. Deshayes, S., Decaffmeyer, M., Brasseur, R., and Thomas, A. (2008) Structural polymorphism of two CPP: an important parameter of activity. *Biochim. Biophys. Acta 1778*, 1197–1205.
49. Ducarme, Ph., Rahman, M., and Brasseur, R. (1998) IMPALA: A simple restraint field to simulate the biological membrane in molecular structure studies. *Proteins 30*, 357–371.
50. Demel, R. A., Geurts van Kessel, W. S., Zwaal, R. F., Roelofsen, B., and van Deenen, L. L. (1975) Relation between various phospholipase actions on human red cell membranes and the interfacial phospholipid pressure in monolayers. *Biochim. Biophys. Acta 406*, 97–107.
51. Lau, S. Y. M., Taneja, A. K., and Hodges, R. S (1984) Synthesis of a model protein of defined secondary and quaternary structure. Effect of chain length on the stabilization and formation of two-stranded α-helical coiled-coils. *J. Biol. Chem. 259*, 13253–13261.
52. Eguchi, A., and Dowdy, S. F. (2009) siRNA delivery using peptide transduction domains. *Trends Pharmacol. Sci. 30*, 341–345.
53. Magzoub, M., and Gräslund, A (2004) Cell-penetrating peptides: small from inception to application. *Q. Rev. Biophys. 37*, 147–195.
54. Wallace, B. A., Lees, J. G., Orry, A. J., Lobley, A, and Janes, R. W. (2003) Analyses of circular dichroïsm spectra of membrane proteins. *Protein Sci. 12*, 875–884.
55. Balayssac, S., Burlina, F., Convert, O., Bolbach, G., Chassaing, G., and Lequin, O. (2006) Comparison of penetratin and other homeodomain-derived cell-penetrating peptides: interaction in a membrane-mimicking environment and cellular uptake efficiency. *Biochemistry 45*, 1408–1420.